Received: 1 August 2018 | Revised: 26 September 2018 | Accepted: 28 October 2018

DOI: 10.1002/eqe.3141

RESEARCH ARTICLE

WILEY

Conceptual seismic design in performance-based earthquake engineering

Gerard J. O'Reilly | Gian Michele Calvi

Scuola Universitaria Superiore IUSS, Pavia, Italy

Correspondence
Gerard J. O'Reilly, Scuola Universitaria Superiore IUSS, Pavia, Italy.
Email: gerard.oreilly@iusspavia.it

Funding information
Italian Ministry of Education, University and Research at IUSS Pavia

Summary

A principal aspect of seismic design is the verification of performance limit states, which help ensure satisfactory behaviour within a performance-based earthquake engineering framework. However, it is increasingly acknowledged that while ensuring life safety is a suitable basic design requirement, more meaningful metrics of seismic performance exist. Expected annual loss (EAL) has gained attention in recent years but tends to be limited to seismic assessment. This article proposes a novel conceptual design framework that employs EAL as a design tool and requires very little building information at the design outset. This means that designers may commence from a definition of required EAL and arrive at a number of feasible structural solutions without the need for any detailed design calculations or numerical analysis. This works by transforming the building performance definition to a design solution space using a number of simplifying assumptions. A suitable structural response backbone is subsequently determined and used to identify feasible building typologies and associated structural geometries. The assumptions made to implement such a conceptual design framework are discussed and justified herein followed by a case study application. This proposed design framework is intended to form the first step in seismic design to identify suitable typologies and layouts before subsequent member detailing and design verification. This way, engineers, architects, and clients can make more informed decisions that target certain performance goals at the beginning of design before further refinement.

KEYWORDS

conceptual design, expected annual loss, performance-based earthquake engineering, storey loss function

1 | INTRODUCTION

Upon the introduction of performance-based earthquake engineering (PBEE) in 1995,[1] seismic design has undergone significant development. PBEE can be simply summarised as foreseeing building damage to different extents for increased levels of seismic shaking. This has evolved into a procedure adopted by most modern design codes, where a number of ground shaking return periods are identified and an acceptable performance associated with each one, typically termed limit states. In design codes such as Eurocode 8 (EC8) in Europe,[2] ASCE 7-16 in the United States,[3] and

 © 2018 John Wiley & Sons, Ltd.

NZS1170 in New Zealand,[4] for example, building performance is checked through the provision of storey drift limits and member verification checks, among other requirements. This of great convenience to engineers since it frames the seismic design problem in terms of familiar quantities like member force or storey drift and can be verified with relative ease using conventional engineering tools. However, when describing the building performance to the owner and its occupants, these quantities have relatively little significance.

From a building owner perspective, what is of immediate interest is the direct financial burden of repairing or replacing their building due to seismic damage. Also of concern are the indirect losses due to building downtime while functionality is being restored. From a building occupant point of view, the safety of the building and the risk of casualty are of more immediate concern. These aspects form part of what has been become known as the Pacific Earthquake Engineering Center (PEER) PBEE methodology initially outlined by Cornell and Krawinkler.[5] This represented an evolution to the initial meaning of the term PBEE whereby performance quantities were framed in a more probabilistic manner. It paved the way for a new definition of building performance using metrics that were of more direct meaning to building owners and occupants, and led to guidelines like FEMA P58[6] being developed. It allows the performance of existing buildings to be quantified in terms of metrics like expected annual loss (EAL) and mean annual frequency of collapse (MAFC), as illustrated in Figure 1. However, this framework and its associated guidelines have mainly been focused on assessment of existing buildings rather than the sizing and design of new ones.

In practice, the seismic design process can be divided into three general phases: (1) the identification of a suitable lateral load-resisting system and its associated geometrical layout, (2) the detailing of structural members for forces and deformations identified using one of many available seismic design methods, and (3) the performance verification of the resulting design with respect to the design requirements using either linear or nonlinear, static, or dynamic analysis. For the second phase, many seismic design methods exist to adequately identify the structural demands for a given definition of seismic input. Similarly for the third phase, where current design codes typically prescribe different performance acceptance criteria defined in terms of strength, stability, and limit state verifications, among others. However, before either of these two phases can be concluded, the lateral load-resisting system and its associated geometrical layout are required. This aspect is not given much attention in current seismic design codes and is generally left to designer experience in consultation with the client's and architect's requirements. Given the key role structural typology plays in the overall performance of a building, it seems logical that some kind of guidance be given to designers who know what kind of performance they and the client require, but are left to an almost trial and error approach—usually refined with experience—when it comes to selecting a structural system.

As noted above, the advances in PBEE have resulted in a methodology that can quantify seismic performance using more advanced metrics. However, it is generally limited to the assessment of existing structures. What is largely absent in PBEE up to now is a comprehensive design framework that can aid designers during the first phase of seismic design,

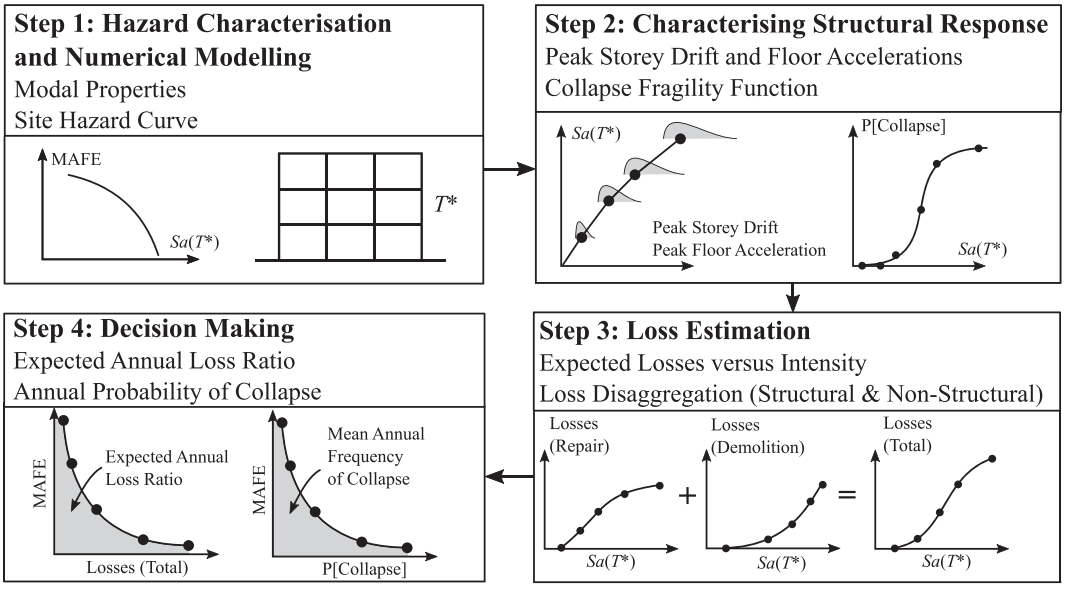

FIGURE 1 Overview of the PEER PBEE framework used to estimate the EAL and MAFC of an existing building (adapted from O'Reilly et al[7]). MAFE denotes mean annual frequency of exceedance, whereas $Sa(T^*)$ refers to the spectral acceleration at a period T^*

where the structure is conceived conceptually or different strengthening measures decided on in the case of retrofitting. Thus, a framework that focuses on the first phase of design, keeping the performance objectives of the third phase closely in mind, whilst utilising the well-developed methods of structural detailing in phase 2, is largely absent. This article outlines a novel framework that addresses this first phase which has largely been left undeveloped, whereby structural systems can be identified utilising more meaningful performance metrics like EAL. By framing the seismic design problem in this manner, it is intended that practitioners can choose more efficient structural systems depending on their respective performance objectives in a more direct and objective manner. This framework may be implemented entirely through the use of a simple spreadsheet and does not require extensive numerical analyses, meaning that it is both intuitive in its application and also easy to revise. The following sections provide an overview of PBEE as stipulated by current design codes, followed by a more rational way to set up the design problem. Using these performance objectives, the proposed design framework is outlined and illustrated via a case study example.

2 | DEFINING ACCEPTABLE PERFORMANCE

2.1 | Design for life safety, check for damage limitation

Current codes tend to define the seismic design problem primarily in terms of ensuring the life safety of its occupants. That is, the procedure is set up so that mitigating collapse becomes the primary objective, whereas ensuring satisfactory performance at frequent levels of shaking is also subsequently checked. These are termed the "no-collapse requirement" and "damage limitation requirement" in the current version of EC8[2] and are suggested to correspond to ground shaking return periods, T_R, of 475 and 95 years, respectively, with possible modifications to account for building importance class. NZS1170, for example, defines two limit states—serviceability and ultimate—within a similar scope and outlines design return periods of 25 and 500 years, respectively, bearing in mind potential modifications for building importance class. ASCE 7-16, on the other hand, outlines a slightly modified approach whereby the building is designed seismic hazard using input defined as a fraction of the maximum considered event (MCE). This seismic hazard input, however, is not related directly to a specific return period of ground shaking but determined from a series of maps outlining risk-targeted spectral values. These spectral values are determined for a target risk of structural collapse of 1% in 50 years using a generic structural fragility curve along with some other adjustments following an approach outlined by Luco et al[8] but recently noted by Vamvatsikos[9] to perhaps not be the most ideal approach. While there are some slight differences in the approaches of the aforementioned design codes, there is one common theme among them all: Structural collapse prevention is of paramount importance.

Following the steps of the lateral force method of analysis specified in EC8 shown in Figure 2, for example, this entails a lateral load-resisting system being chosen by the designer, its behaviour factor, q, identified based on its expected level of global ductility, and the design forces determined based on some empirical estimate of initial period, T_1. These design forces are subsequently used to size and detail the structural members of the chosen lateral load-resisting system. Other performance objectives like the peak storey drift (PSD) demands, θ, at other more frequent levels of ground shaking are subsequently checked in a relatively straightforward manner. However, a number of problems

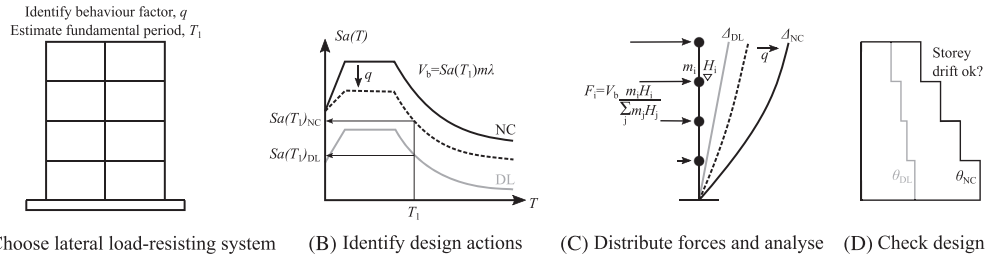

FIGURE 2 Basic steps of FBD as prescribed by the current version of EC8, where (A) the lateral load-resisting system is chosen, (B) design actions are identified for no-collapse (NC) and damage limitation (DL) requirements, where the NC actions are reduced by the behaviour factor, q, and $m\lambda$ is an estimate of the participating mass in the first mode. Using these design actions, the structure is sized using the design lateral forces, F, distributed in (C) and the drift demands, θ, are checked for suitability in (D)

exist not only with this philosophy of designing structures but also with the way in which performance objectives are being met.

The design philosophy whereby design forces are determined using empirical estimates of initial period and unique behaviour factors (ie, the anticipated ductility capacity) are assumed for structural systems presents its own inherent problems. This approach has become known as force-based design (FBD), due to forces being the quantity that drive the procedure, and its limitations have been well documented in the literature, most notably by Priestley.[10] It results in a design process whereby the design quantity of interest (ie, displacement demand, D) is checked to be less than some prescribed limit or capacity, C, meaning D/C simply needs to less than one. Thus, there is no real differentiation between solutions that grossly overdesign (ie, $D/C = 0.2$) and solutions that fall just inside the acceptance criteria (ie, $D/C = 0.99$). This is not to suggest that engineers do not strive to achieve design efficiency but rather to highlight that the code acceptance criteria do not strictly require them to and overdesigns may result in the name of conservatism and safety. The consequence of this is that the performance of two structures designed by different engineers with differing attitudes to design efficiency, characterised via the PEER PBEE framework shown in Figure 1, will greatly differ despite them both satisfying the same initial design criteria.

Displacement-based design (DBD) was proposed as an alternative to FBD, whereby the displacement demand is set as the prescribed limit or capacity (ie, $D = C$) at a certain level of seismic shaking as illustrated in Figure 3. This gave a simple and direct method of seismic design which culminated in the development of direct displacement-based design (DDBD) described in Priestley et al.[11] This was proposed as a suitable alternative to FBD as it possesses advantages not only in terms of design approach and structural reasoning of the problem but since it is better aligned for the objectives of PBEE, whereby performance levels can be linked to levels of structural demand and damage for different levels of shaking, rather than forces.

Regardless of which approach is used to arrive at a design characterised by a lateral load-resisting system and its associated member capacities, some aspects of how building performance at other levels of seismic shaking is safeguarded tend to be left wanting. This arises from how design methods are inclined to be set up to provide life safety at a single intensity of shaking and subsequently check the other limits as secondary aspects. For example, EC8 describes how the no-collapse requirement can be considered satisfied if the design action is less than the design resistance along with some other requirements regarding ductility, stability, and capacity design. The damage limitation requirement is then considered satisfied if storey drift limits are met, whose values range between 0.5% and 1.0% depending on nonstructural element typology and building importance class. Similar requirements are set forth in New Zealand's NZS 1170, albeit with slightly different terminology, but the basic concept remains the same. In the US, ASCE7-16 requires the storey drift to be limited to prevent structural collapse in a more risk-targeted manner but does not explicitly require any design adjustments to mitigate damage at more frequent levels of ground shaking. The first issue regarding the no-collapse requirement has been discussed previously, but the protection of damage to nonstructural elements via storey drift limits is examined further here. While damage to some nonstructural elements is closely related to storey drift demands at frequent levels of shaking, these only make up a portion of the potential source of economic losses. For example, Taghavi and Miranda[12] have shown how a significant portion of loss is associated with acceleration-sensitive components, meaning that modern design codes offer no direct protection at the design stage for such elements. Furthermore, the storey drift limits currently in place in EC8, for example, have been shown by Welch and Sullivan[13] to be rather ineffective at mitigating damage to interior gypsum partitions when assessed using a

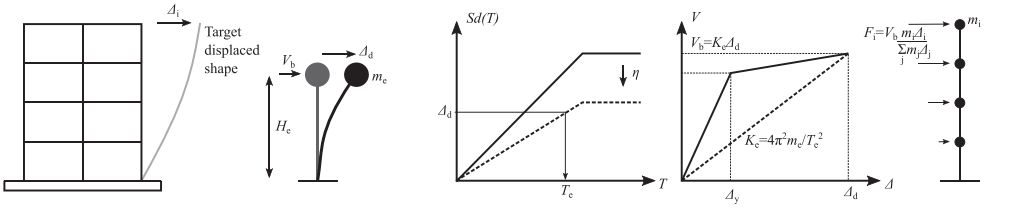

FIGURE 3 Basic steps of DDBD,[11] where a lateral load-resisting system is chosen and target lateral displacement profile set in (A), and equivalent single degree of freedom (SDOF) system identified in (B), whose effective period, T_e, is found in (C). This is used in (D) along with the design displacement, Δ_d, to identify the design base shear, V_b, which is then used to distribute the lateral forces, F, and size the structural members

PEER PBEE-oriented approach. Furthermore, a major problem with most design methods and codes that exist in current practice is that the probabilistic aspects are ignored and the uncertainty in structural response is not propagated fully to give more risk-consistent designs. This has been previously discussed by Vamvatsikos et al[9,14] and will be revisited here in Section 3.2. Lastly, it is noted that one of the first steps prior to using either FBD or DDBD is to identify a lateral load-resisting system and building geometry. It has already been noted that while this is a primary step in the seismic design process, design codes do not provide any indication on suitable choices of lateral load-resisting system at the outset of the design process.

2.2 | Using EAL as a design tool

The points raised above indicate the need for design approaches more in line with the PEER PBEE framework. This is so that the performance of a newly designed building can be verified in a more consistent manner, whilst also considering both PSD and peak floor acceleration (PFA) sensitive nonstructural elements and the lateral load-resisting system. The simplest solution would be to adapt current design methods to account for these. But how? FBD is a simplified design process whereby a lateral force is identified and designed for, where PSD and PFA demands are then evaluated, with subsequent iterations if required. As Priestley et al[11] noted, DDBD is a direct method focusing on PSD demands to make it more suited to PBEE. Therefore, should it be possible to extend DDBD to account for PSD and PFA demands in a more direct manner, this would be a significant improvement.

The focus herein is on how performance objectives are actually established. That is, how can the performance of a building defined using more advanced measures be translated into design quantities? EAL has been predominantly used in assessment and forms part of the seismic classification framework recently introduced in Italy.[15] This framework initially postulated by Calvi et al[16] proposed EAL as a metric that can be used to classify a building's seismic performance. It is analogous to the energy consumption scale used in Europe that provides a simple and objective way to quantify the relative performance of different electrical appliances. Again, this framework was primarily targeted toward the assessment of existing buildings and provides a metric with which improved performance can easily be demonstrated, but its general implications were clear: EAL may be used in the seismic design and assessment process. The use of expected losses within the broader goal of providing improved performance was also outlined by Krawinkler et al,[17] where a framework to find a design solution by controlling the expected losses at specific return periods was developed. This aspect is pursued further here, albeit in a slightly different manner, since many of the steps outlined by Krawinkler et al[17] require vast amounts of analysis to be carried out in order to provide the necessary ingredients for the framework, with iteration and rerunning of analysis often needed. Here, a more simple and direct approach is sought whereby designers can easily arrive at a set of feasible design solutions based on some target value of EAL.

3 | PROPOSED FRAMEWORK

3.1 | Overview

The basic flow of the proposed procedure is described herein and is separated into two distinct parts: (1) identification of performance requirements and (2) identification of feasible structural solutions. The first part can be summarised as follows:

1. Identify site hazard: source size hazard information and uniform hazard spectra (UHS) for different return periods.
2. Define performance objectives: establish a design loss curve in terms of EAL characterised by an expected loss ratio, y, and the corresponding mean annual frequency of exceedance (MAFE), λ, for a number of limit states.
3. Identify design spectra: using the MAFE for each limit state, λ, the return periods of the UHS to be designed for, T_R, are identified while also accounting for response uncertainty.
4. Identify storey loss functions: knowing the building occupancy type, identify a set of storey loss functions that relate expected monetary losses to design parameters like the maximum PSD, θ_{max}, and maximum PFA, a_{max}, along the height of the building.
5. Identify acceptable design limits: using the performance objectives defined in step 2 and the storey loss functions in step 4, identify acceptable structural design limits, θ_{max} and a_{max}, for each limit state.

Knowing these acceptable values of θ_{max} and a_{max} at each limit state, feasible design solutions can be identified in the second part as follows:

1. Define building information: establish fundamental building information like the number of storeys, seismic mass, and storey heights.
2. Convert θ_{max} and a_{max} at the serviceability limit state: identify spectral displacement and acceleration limits for the serviceability limit state (SLS), $\Delta_{d,SLS}$ and α_{SLS}, respectively.
3. Identify feasible initial secant to yield period range: using the performance criteria $\Delta_{d,SLS}$ and α_{SLS} computed in step 2, establish a range of permissible initial secant to yield periods.
4. Trial lateral strength and identify demand: trial a value of lateral strength at the ultimate limit state (ULS), α_{ULS}, and identify the design displacement, $\Delta_{d,ULS}$, using the same process as step 2.
5. Estimate spectral capacity: knowing that for a structure responding with a reasonable degree of nonlinearity at the ULS, its spectral reduction factor will tend to $\eta \approx 0.60$ for most structural systems. Use this as an initial starting point in conceptual design and check to ensure compatibility between the α_{ULS}, $\Delta_{d,ULS}$ and the assumption of η with respect to the design spectrum.
6. Identify yield displacement and check period: knowing the design displacement at the ULS, $\Delta_{d,ULS}$, compute the maximum permissible yield displacement by simply dividing by approximately 2.5, which corresponds to the ductility beyond which the displacement modification factor, η, tends to stabilise to around 0.60 for most structural systems. Set a design yield displacement, Δ_y, less than this limit and compute the initial secant to yield period of the system. Check if it respects the limits set forth earlier. If not, revise lateral strength.
7. Identify suitable structural geometry: from the established yield displacement, Δ_y, and recognising that the yield displacement is a function of structural geometry and material properties, identify a suitable structural geometry for conceptual design.
8. Identify design lateral forces and design system: convert the design lateral strength, α_{ULS}, into a design base shear, V_b, and distribute along the height to give design lateral force profile.

This framework serves as an initial screening for suitable designs that can be performed prior to fully detailing and verifying the structure. Each of the above steps is discussed in the following subsections to provide further background and justification followed by a case study implementation in Section 4.

3.2 | Identification of building performance requirements

3.2.1 | Identify site hazard

One of the first steps in seismic design is to identify the site hazard and suitable seismic input. Different methods exist to do this, such as utilising code-defined spectra or the results of probabilistic seismic hazard analysis. Other more novel ways of defining design spectra have also been proposed by Calvi[18] year, for example. These aspects are beyond the scope of this article but suffice to say that whichever approach is used, the resulting design spectra ought to be a UHS.

3.2.2 | Define building performance objectives

To identify structural performance limits using EAL, consider the expected loss ratio (ELR), y, versus MAFE, λ, shown in Figure 4. ELR is the expected value of direct monetary losses arising from building damage normalised by its replacement cost. MAFE is the mean annual frequency of a limit state being exceeded and should not to be confused with the mean annual frequency of exceeding a certain level of ground shaking (ie, a site hazard curve) discussed further in Section 3.2.3. While the number and definition of limit states vary slightly from one design code to the next, the basic concept is essentially the same: to mitigate damage during frequent events and maintain life safety during rare events. To maintain a level of generality with respect to different design codes, three limit states are utilised herein: fully operational limit state (OLS), serviceability limit state (SLS), and ultimate limit state (ULS). SLS and ULS are aimed at ensuring satisfactory performance at lower and higher levels of ground shaking, respectively. The OLS performance point describes the point when direct monetary losses begin to accumulate due to building damage. These are shown in Figure 4 with respect to their anticipated ELR and MAFE. Based on qualitative performance expectations, ELRs may

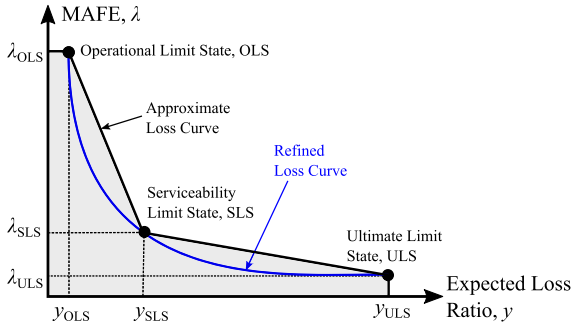

FIGURE 4 Illustration of approximate and refined loss curves, where integrating the expected loss ratio, y, with MAFE, λ, using the approximate loss curve is used to establish the design EAL shaded in grey. The vertical axis is plotted using a logarithmic scale for illustration purposes [Colour figure can be viewed at wileyonlinelibrary.com]

be tentatively defined as $y_{OLS} = 1\%$, $y_{SLS} = 15\%$, and $y_{ULS} = 100\%$, for example. The OLS and ULS points describe the points at which the building begins to accumulate monetary loss and where the ELR saturates at the building replacement cost, respectively. Referring to the seismic classification guidelines recently introduced in Italy,[15] which were compiled based on building loss data collected following the 2009 L'Aquila earthquake,[19] these ratios are deemed representative given their qualitative descriptions. Defining a nonzero value of y_{OLS} recognises that while losses may be induced for very small events, there will typically be a lower bound threshold below which insurers will not pay out premiums. While a value of 1% is set here, further studies may look to refine this value using both numerical analysis and data from past events. Adopting a value of $y_{ULS} = 100\%$ implies that the building has sustained losses to the extent that it is completely unrepairable and must be replaced but is distinct from the complete collapse of the building of the structure resulting in the loss of life. Lastly, the value of y_{SLS} tentatively proposed here is aimed at defining the point at which the building starts to accumulate significant loss (ie, >10%). This value of 15% is in line with the value proposed for the Italian seismic classification guidelines at the "damage limitation" limit state. Again for completeness, the ELR values discussed above refer exclusively to direct monetary losses. Indirect losses are not considered here, but their potential inclusion in such a framework is discussed further in Section 5.4.

Figure 4 is noted to possess just three performance points, whereas other approaches[15,20] tend to use more. This simplification is made in recognition that while more performance points on the approximate loss curve shown in Figure 4 may be desirable, a balance between simplicity and accuracy is sought. In Figure 4, the EAL may be approximated as the area beneath the approximate loss curve and is shaded in grey. This is termed approximate as more points may be added to give a more refined curve, like that shown in blue. This aspect requires careful consideration since while the difference in area between the approximate and refined loss curve may appear insignificant, this is a result of the log scale of the vertical axis in Figure 4. In fact, it can be easily shown that this overestimation in the area between the two curves can result in an EAL overestimation of up to 50% when compared with the refined curve. This overestimation may be overcome using a closed-form expression with the same functional form of the refined loss curve. A logical starting point would be the seismic hazard curve fits [eg,[21]] described as follows:

$$\lambda = c_0 \exp\left[-c_1 \ln y - c_2 \ln^2 y\right] \tag{1}$$

where the coefficients c_0, c_1, and c_2 can be simply fitted to pass through the three limit state points shown in Figure 4. The EAL is then evaluated as the area beneath this closed-form expression and is anticipated to be much more representative of the actual EAL computed using more refined analysis. Compared with loss curves from previous studies [eg,[7,22]], this functional form has been seen to be representative of the general shape of a typical loss curve.

Computing the design EAL of the building this manner, its seismic performance is quantified in a more meaningful way. This is through the definition of an acceptable value of ELR at each limit state and the computation of a design EAL using Equation 1. The value of EAL that would be deemed acceptable is a decision left to the building owner or different stakeholders, but the D.M. 58/2017 guidelines recently introduced in Italy provide a tentative scale for guidance. While the computation of EAL using a refined loss curve described by Equation 1 using ELR values for the chosen limit states has been outlined, the MAFEs associated with each limit state are yet to be established and are discussed in the following section.

3.2.3 | Identify design spectra

In the past, limit state MAFE has typically been assumed to correspond to the reciprocal of the return period for which it was designed. Doing this, however, equates the ground shaking exceedance rate (ie, the site hazard curve, H) and limit state MAFE in a risk-inconsistent manner. Essentially, it implies that the problem is deterministic and that there is no variability at any stage of the PEER PBEE integral, which is not the case. This is not to say that any solution designed in this manner is inherently unsafe since design codes do foresee a number of safety factors at various stages of the design process but rather to point out that their actual performance quantified via limit state MAFE in a more thorough and risk-consistent manner remains relatively unknown. This aspect has been explored in more detail in a recent project in Italy,[23] which the interested reader is referred to for more details. A closed-form solution for the MAFE of a limit state is described by Cornell et al[24] as

$$\lambda = H(\widehat{s}) \exp\left[0.5k_1^2\beta^2\right] \tag{2}$$

where $\widehat{s}$ is the median value of the intensity measure, s, for a given limit state exceedance, k_1 is a site hazard term, and β is the dispersion related to the limit state intensity. For example, Pinto and Franchin[25] pointed out that λ can be expected to be ~2.25 times greater than $H(\widehat{s})$ for some typical values of the β and k_1 terms in Equation 2, but noted that this ratio is expected to vary with limit state and also site hazard conditions. This is illustrated in Figure 5, whereby the overall impact is that there is a general shift upward of the MAFE due to the amplification of λ with respect to $H(\widehat{s})$.

The approach utilised herein is to adopt a set of return periods for each limit state and approximate the MAFE using Equation 2. These return periods are initially set following the requirements of the revised draft of EC8,[26] with 60 and 1600 years being adopted as starting values for the SLS and ULS limit states, respectively. For the OP limit state, a value of 10 years is adopted, following the D.M. 58/2017 guidelines in Italy.[15] Utilising these proposed values of limit state return period, the MAFE is computed using Equation 2 and the design EAL from Equation 1. If this value is deemed to be unsatisfactory, the value of λ should be modified accordingly and the required return period of ground shaking, T_R, can be back-calculated by inverting Equation 2. It is recognised that this is an approximation that depends heavily on the assumed values of k_1 and β, but it is simply proposed as a starting point that may be subsequently revised. While the design return periods of each of the limit states may be modified to account for the different building performance needs, the minimum values of ground shaking stipulated by the design code should also be respected.

3.2.4 | Identify storey loss functions

Once the SLS and ULS points have been identified, these are used to identify suitable maximum PSD, θ_{max}, and PFA, a_{max}, limits for design. To do this, information relating the accumulation of direct monetary losses with respect to increasing structural demand are required. Ramirez and Miranda[27] have proposed such a solution, termed storey loss functions, whereby the damageable elements are divided into distinct element groups. Exemplary functions are shown in Figure 6 for different building occupancy types, where the ELRs of PSD-sensitive structural elements, $y_{S,PSD}$, PSD-sensitive nonstructural elements, $y_{NS,PSD}$, and PFA-sensitive nonstructural elements, $y_{NS,PFA}$, are illustrated. These are

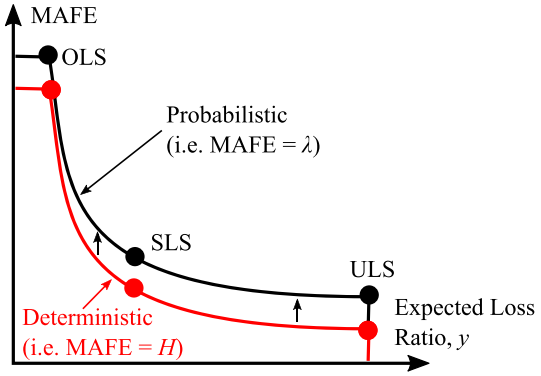

FIGURE 5 Impact of considering the limit state exceedance in a deterministic or probabilistic fashion [Colour figure can be viewed at wileyonlinelibrary.com]

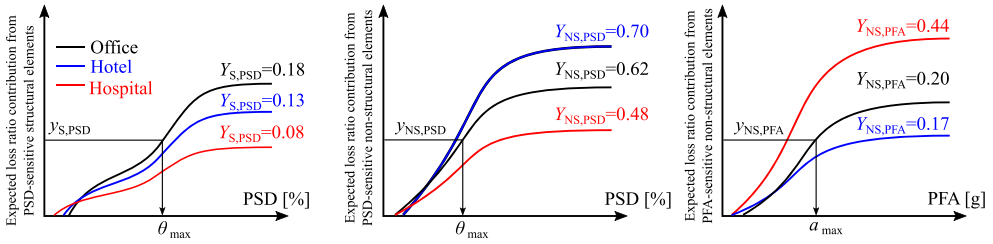

FIGURE 6 Identification of limit state design parameters using storey loss functions. For illustration, relative cost proportions of different damageable element groups adopted from Taghavi and Miranda[12] for different occupancy types [Colour figure can be viewed at wileyonlinelibrary.com]

expressed as a ratio to the saturating direct loss of each damageable group of a single storey in Figure 6, Y, which total unity (ie, $Y_{S,PSD} + Y_{NS,PSD} + Y_{NS,PFA} = 1.0$) and corresponds to the proportion, or weighting value, of each element group. It also means that all structural damage is related to PSD alone and the nonstructural damage to either PSD or PFA. Other demand parameters such as floor velocity may be considered but are beyond the scope of this work.

For what concerns the availability of such storey loss functions, Ramirez and Miranda[27] provided a set to evaluate low to high-rise office buildings in California, whereas some more recent work by Papadopoulos et al[28] looked at developing similar functions for steel buildings in Greece. Due to the nature of a building's damageable elements, their expected relative quantities and repair costs mean that while the functional form of these curves shown in Figure 6 will typically be similar, the assumptions and data used in their development means that they tend to be region-specific. Such functions are not widely available but the advent of the FEMA P58 guidelines and its associated tools mean that they are becoming more feasible to generate.

3.2.5 | Identify acceptable design limits

To link the ELR at each limit state illustrated in Figure 4 to a structural demand parameter via the storey loss functions illustrated in Figure 6, some assumption needs to be made regarding the relative weights, Y. For example, take a single-storey structure designed not to exceed the specified ELR at a certain limit state. This means that the ELR at that performance limit state is described by

$$y_{S,PSD} + y_{NS,PSD} + y_{NS,PFA} = y \tag{3}$$

which is the sum of all sources of loss. From Equation 3, the following can be written

$$y_{S,PSD} = yY_{S,PSD}, \quad y_{NS,PSD} = yY_{NS,PSD}, \quad y_{NS,PFA} = yY_{NS,PFA} \tag{4}$$

meaning that the individual values of damageable element group loss (ie, $y_{S,PSD}$, $y_{NS,PSD}$, and $y_{NS,PFA}$) to be entered into the respective subplots of Figure 6 can be computed as a product of the target ELR, y, and the relative weighting, Y. By entering the vertical axes Figure 6A to 6C, these will return two values of θ_{max} and a single value of a_{max} not to be exceeded in order to maintain that level of expected loss. Taking the smaller of the two θ_{max} values, which will in most cases be that associated with $y_{NS,PSD}$, the design demand parameters are therefore established.

3.3 | Identification of feasible structural solution

Having defined acceptable building performance in Section 3.2, the task remains to arrive at a feasible structural solution. Note that this implies more than one design solution (ie, lateral strength, stiffness, and ductility) and structural system (ie, RC frame, RC wall, steel braced frame) may be possible for the design constraints identified in Section 3.2.2. Potential solutions can be identified this way without committing to a specific lateral loading system. This aspect is particularly useful in aiding the conceptual seismic design stage of the construction process, where engineers present architects and clients with a range of suitable structural systems they are confident will work within the given seismic performance constraints but have not yet conducted any detailed analysis.

3.3.1 | Define building information

The first stage of any design process is to have some basic building information. At this point, very little information is required since it is still at the conceptual design stage. However, to permit this conceptual design, information regarding the number of storeys, storey heights, and seismic weight of each floor is required. Since the structure is still being conceptually designed, the total weight of each floor is not yet known. The live load is given by the design code, but the dead load is mainly a function of the slab system, which has not yet been decided. A trial dead load value may be adapted to be combined with the live load, but it is noted that this too may become a design variable to be optimised at this conceptual stage of design. For instance, designers may preliminarily investigate the usage of more advanced lightweight slab systems to reduce the dead load instead of heavier traditional slabs systems when excessive mass becomes a problem.

3.3.2 | Identify spectral values at SLS

The next step is to convert the maximum PFA, $a_{\max}$, and maximum PSD, $\theta_{\max}$, to spectral accelerations and displacements, which are denoted α_{SLS} and $\Delta_{\mathrm{d,SLS}}$ for the SLS, respectively. Starting with PSD, an equivalent SDOF system is employed to characterise a first-mode dominated multidegree of freedom (MDOF) system. This is similar to the approach adopted in DDBD where the displacement of the equivalent SDOF system is given by

$$\Delta_d = \frac{\sum_{i=1}^{n} m_i \Delta_i^2}{\sum_{i=1}^{n} m_i \Delta_i} \tag{5}$$

where n is the number of floors in the building, with mass m_{i} at each floor level i and the displaced shape is denoted as Δ_{i}. While the floor mass is known, the displaced shape is structural system-dependant. For typical structural systems illustrated in Figure 7, these displaced shapes are described in Priestley et al[11] as follows:

$$\text{RC Frames } \Delta_i = \omega_\theta \theta_{max} H_i \left(\frac{4H_n - H_i}{4H_n - H_1} \right) \tag{6}$$

$$\text{RC Walls } \Delta_i = \omega_\theta \begin{cases} \dfrac{\theta_{max} H_i^2}{H_n} \left(1 - \dfrac{H_i}{3H_n} \right), & \mu < 1 \\ \dfrac{\epsilon_y H_i^2}{l_w} \left(1 - \dfrac{H_i}{3H_n} \right) + \theta_p H_i, & \mu \geq 1 \end{cases} \tag{7}$$

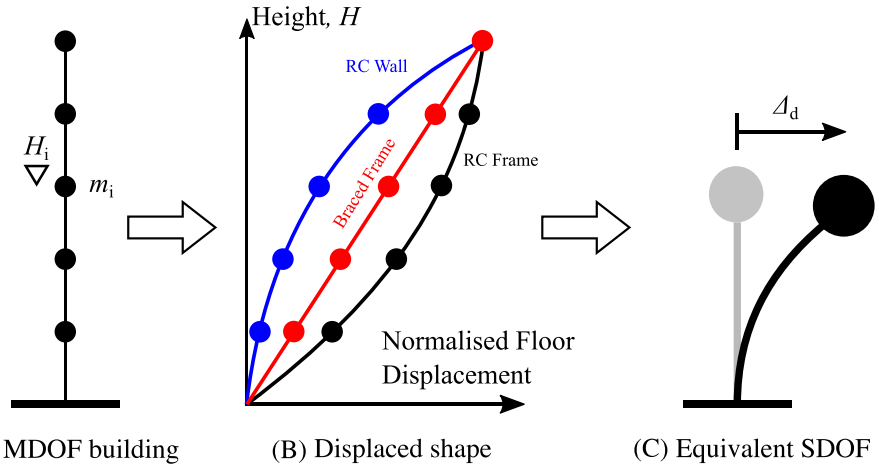

FIGURE 7 Identification of Δ_{d} for different structural systems [Colour figure can be viewed at wileyonlinelibrary.com]

$$\text{Braced Frame } \Delta_i = \omega_\theta \theta_{max} H_i \tag{8}$$

where μ is the level of ductility, H_i is the ith floor's elevation above the base, ε_y is the yield strain of the reinforcement, l_w is the RC wall length, θ_p is the rotation capacity of the plastic hinge formed at the RC wall base, and ω_θ is a reduction factor included for the possible storey drift amplification due to higher modes of vibration. In the case of RC frames and braced frames, it is assumed for simplicity here that these displaced shape expressions are representative at all damage states. Therefore, for a given value of θ_{max}, the corresponding Δ_i can be found and subsequently the Δ_d for each structural system. At the SLS where no ductile behaviour is anticipated, the values of $\Delta_{d,SLS}$ are computed.

Relating PFA to spectral acceleration, Sa, is a little trickier due to the nature of the problem where unlike θ_{max}, a_{max} cannot be assumed to be first mode dominated. Furthermore, methods to estimate floor accelerations in buildings such as Calvi and Sullivan,[29] among others, rely on knowing the fundamental periods of vibration and associated mode shapes a priori. However, since the process of identifying a Sa for various building solutions assumes that the structure remains in the elastic range of response, some simplifications can be made. Consider that the jth mode contribution to the PFA at the ith floor for an elastically responding structure to be

$$a_{i,j} = \phi_{i,j} \Gamma_j Sa(T_j) \tag{9}$$

where $Sa\ (T_j)$ is the spectral acceleration at the jth mode period of vibration, $\varphi_{i,j}$ is the jth mode shape value at floor i, and Γ_j is the jth mode's participation factor, given by

$$\Gamma_j = \frac{\sum_i m_i \phi_{i,j}}{\sum_i m_i \phi_{i,j}^2} \tag{10}$$

Combining the first few modes using a square root sum of the squares (SRSS) combination gives the PFA profile along the height, a_i, with a maximum value of a_{max}. Knowing the structural typology as any one of those illustrated in Figure 7, it will tend to have relatively standardised mode shapes, meaning that for a building with a known number of storeys, the individual Γ values will remain somewhat constant since they depend on storey stiffness and floor mass distribution. This means that by knowing the number of storeys and the structural typology, the various terms in Equation 10 can be simplified and approximated by a single coefficient γ defined as

$$\alpha_{SLS} \approx \gamma a_{max} \tag{11}$$

It is noted that a number of simplifying assumptions need to be made in order to arrive at such a simple relation and it is also recalled that this is not intended as a substitute for estimating actual PFA values in existing buildings. In fact, one may consider it to be a simplified version of the approach outlined by FEMA P-58, where PFA is empirically related to the input ground shaking for different structural typologies, albeit in terms of PGA acceleration whereas $Sa(T_1)$ is utilised here. Initial parametric studies on the elastic modal properties of structures suggest values of γ for low-rise structures to be of the order of 0.70 to 0.80, 0.75 to 0.90, and 0.65 to 0.80 for RC frames, RC walls, and braced frames, respectively. Future work should look to refine these coefficients for different typologies of differing number of storeys but for the purposes of conceptual design discussed here, they are deemed reasonable.

3.3.3 | Identify feasible initial secant to yield period range

Using the values of $\Delta_{d,SLS}$ and α_{SLS} identified in Section 3.3.2, these can be marked on the design SLS spectrum as shown in Figure 8, which results in a range bound by the two lines from the origin. Recalling that the slope of a line through the origin is directly related to the period of vibration, T, it becomes clear that in order to respect the SLS requirements, the eventual design solution must possess a first-mode period, T_1, within the zone highlighted in grey and bound by points 1 and 2 in Figure 8. This essentially implies that the structure must be stiff enough to not exhibit excessive deformation but be flexible enough so as not to generate excessive floor accelerations at the SLS.

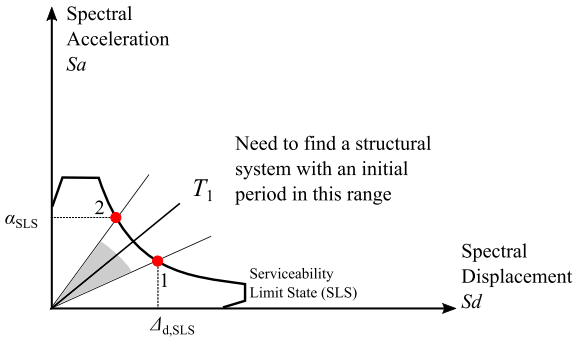

FIGURE 8 Identification of permissible initial secant to yield period range based on PFA and PSD limits for the SLS [Colour figure can be viewed at wileyonlinelibrary.com]

3.3.4 | Trial lateral strength and identify ULS demand

With the permissible period range known from Figure 8, two further pieces of information are required: the design displacement and the lateral strength. The lateral strength can be directly related to *Sa* by assuming first-mode dominated response, shown in Figure 9 as α_{ULS}, and is set as a trial value by the designer. This approach differs from existing design methods where determining the design lateral force is seen as the holy grail, whereas here it is a relatively flexible parameter that must simply respect certain conditions. Examining the latter aspect of design displacement, this was discussed previously in Section 3.3.2 where the value of θ_{max} identified in Section 3.2.5 for the ULS can be converted to a design displacement, $\Delta_{d,ULS}$, using an approach similar to Section 3.3.2. This value of $\Delta_{d,ULS}$ is illustrated via point 3 and the area bound by points 1, 2, and 3 in Figure 9 represents the design solution space within which the final backbone behaviour must fall.

3.3.5 | Compute required spectral capacity

At the ULS, the effects of system nonlinearity need to be accounted for. Considering the effective period, T_e, passing from the origin through point 3 and comparing this expected capacity with the elastic spectral demand marked at point 4 in Figure 9, $Sd\,(T_e)$. The nonlinear behaviour of the structure will be expected to account for this amplification in the structure's spectral capacity. The relationship between linear and nonlinear behaviour in seismic design may be found via a modification to the elastic design spectrum by reducing or overdamping as a function of ductility, as shown in Figure 9. Other approaches, such as the use of inelastic spectra advocated by Miranda[30] or Vidic et al,[31] for example, may also be employed to relate the nonlinear response and linear analysis but for brevity are not included here. Since the design displacement, $\Delta_{d,ULS}$, and the elastic response spectrum are known, this required amplification of the structure's spectral capacity with respect to the elastic demand due to the nonlinear behaviour is simply determined as

$$\eta = \frac{\Delta_{d,ULS}}{Sd(T_e)} \tag{12}$$

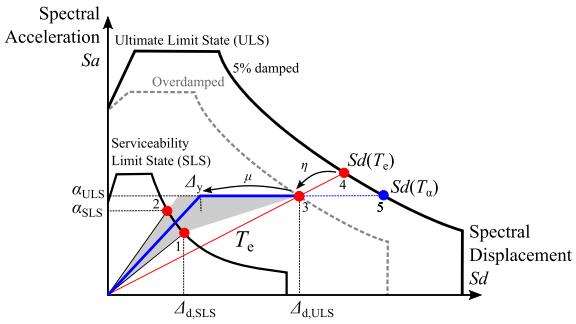

FIGURE 9 Identification of design solution space shaded in grey considering the permissible period range and the trialled value of lateral strength capacity [Colour figure can be viewed at wileyonlinelibrary.com]

These are typically referred to as displacement reduction factors in the literature but are herein referred to as displacement *modification* factors (DMFs). Priestley et al[11] outline a number of expressions for various structural systems characterised by different hysteretic models representative of different structural systems. Such relationships are plotted in Figure 10 using expressions proposed by Priestley et al[11] and O'Reilly and Sullivan,[32] for example. Using these kinds of plots, the required ductility, μ, can be identified by entering from the vertical axis with the required spectral modification factor, η, and reading off the corresponding value. For cases where the required η does not intersect the curve (eg, $\eta = 0.50$), this essentially implies that the structural system being examined is simply not capable of providing sufficient spectral reduction to sustain such a demand and the trial lateral strength needs to be modified. However, one may notice that beyond $\mu \approx 2.5$, η tends to stabilise to ≈0.60. This can be seen further when examining the results of numerous different quantification studies[33-35] looking at the relationship between the inelastic displacement and the spectral displacement at the effective period of different hysteretic systems. Therefore, in a preliminary design situation where a reasonable level of ductility is anticipated for a new structure, it is reasonable to assume a value of $\eta = 0.60$. Checking this assumption with respect to the ULS point and elastic design spectrum (points 3 and 4 in Figure 9), the initial choice of lateral strength can be evaluated and modified to respect compatibility. Once the permissible initial period range has been established and the target displacement identified at the SLS and ULS, respectively, the minimum μ required from the system is used to work back to find the yield displacement of the system, Δ_y, as shown in Figure 9. By assuming a preliminary design value of $\eta = 0.60$, this implies that the structure must exhibit a μ greater than 2.5. Otherwise, the more refined value of μ required for a different value of η may be found using plots such as those in Figure 10, as previously mentioned.

The above discussion has utilised the spectral reduction approach advocated by Priestley et al[11] to account for system nonlinearity, where the relationship is characterised using the ratio of elastic spectral demand at the effective period to the design displacement. In such an approach, the effective period, T_e, is being preserved but, when considered further, can be found to have little meaning with respect to the response of the actual structure (ie, T_e is a proxy used to characterise response but does not have a physical meaning). Expressions such as those in Figure 10 derive from the mean results of many nonlinear response history analyses on simplified SDOF models and possess a great degree of variability. By conserving T_e in Figure 9, for example, and accepting that the value of η may be slightly larger or smaller due to its inherent variability, this means that the spectral reduction will be returning a value of *Sa* that does not coincide with point 3 on Figure 9, but somewhere close and along the red line shown. For an equivalent elastic system responding at T_e, this makes sense as it is in line with the initial assumptions, but if considered from a more realistic point of view, can be somewhat bemusing. This is because the response being predicted is conserving T_e—a proxy value—and returning varying values of lateral strength characterised by a spectral acceleration capacity in Figure 9, α_{ULS}. In assessment, where the response of a structure is given as the blue backbone in Figure 9, having different values of lateral strength distributed along the effective period line because of the inherent variability in η does not make physical sense and is not what the actual structure would do. Instead what would happen is that the structure, analysed using a set of ground motions all conditioned to the same value at *Sa* (T_e), would be responding along the horizontal line from point 3 toward point 5, assuming no strength degradation. This implies that the lateral strength should be conserved instead of the period of the system, which would result in a drastic shift from the current thinking of DMFs. Doing so would result in a new breed of DMFs that would be defined as a ratio of $\Delta_{d,ULS}$ to the spectral demand, *Sd* (T_α) described by

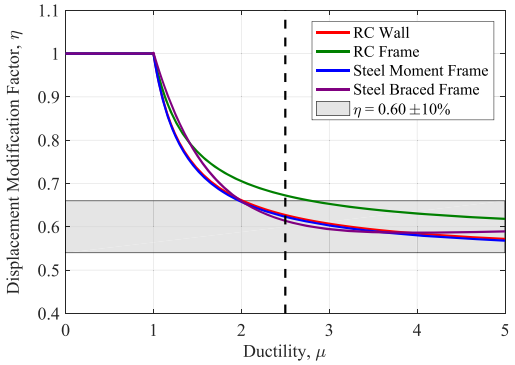

FIGURE 10 Displacement modification factors for some typical structural systems, where the value of η can be seen to stabilise beyond a $\mu \approx 2.5$ [Colour figure can be viewed at wileyonlinelibrary.com]

$$\chi = \frac{\Delta_{d,ULS}}{Sd(T_\alpha)} \tag{13}$$

marked at point 5 in Figure 9. From a general design and assessment philosophy, such a change in the approach would neither be following classical DBD, which utilises the response at T_e, nor would it be following FBD, which conserves the initial period, T_1. This aspect is not developed further here but is noted as a potential future development to the proposed framework to be investigated further considering the findings and observations of past work by studies such as Miranda and Ruiz-García.[36] While such a future development would inevitably result in a modification to the proposed design framework, this would merely be in terms of switching the usage of the terms η and χ, whereas the overall structure and flow of the method would remain unchanged.

3.3.6 | Identify yield point and check initial secant to yield period

Knowing the value of η and its associated μ, the yield spectral displacement, Δ_y, of the structural system is computed as follows:

$$\Delta_y = \frac{\Delta_{d,ULS}}{\mu} \tag{14}$$

meaning that the final bilinear backbone of the structural system has been identified and is illustrated via the blue line in Figure 9. It is noted that the value of μ used in Equation 14 may also be determined from Figure 10 but can be taken as ≈2.5 initially. This backbone assumes that the second-order geometry effects, or P-Delta effects, are balanced out by the postyield hardening of the structure to result in an elastic-perfectly plastic system, although these issues may be considered in further detail in the future, also acknowledging that this is a conceptual point of design.

3.3.7 | Identify suitable structural geometry

As outlined in Figure 9, the design outputs from the proposed approach are α_{ULS}, μ, and maximum Δ_y required to maintain compatibility with the identified performance objectives. α_{ULS} and μ are simply related to the provided strength of the dissipative zones in the eventual structural design, whereas Δ_y is related to the chosen structural system. Knowing Δ_y, the final dimensions and material properties of the structural system can be identified since it is well known to be independent of the lateral strength.[10]

Take an RC frame with a ductile beam-sway mechanism, for example, the yield drift, θ_y, has been shown by Priestley et al[11] to be given by

$$\theta_y = \frac{0.5\epsilon_y B}{h_b} \tag{15}$$

where B is the bay width of the frame and h_b is the beam depth. In the case of steel moment frames, Priestley et al[11] noted that the coefficient in Equation 15 could simply be changed to 0.65. This can be then related to the Δ_y of the equivalent SDOF through the following relationship:

$$\Delta_y = \theta_y \frac{\sum_{i=1}^{n} m_i \Delta_i H_i}{\sum_{i=1}^{n} m_i \Delta_i} \tag{16}$$

where the expression describing the displaced shape was outlined in Equation 6 above. Therefore, by knowing the required Δ_y of the equivalent SDOF from Section 3.3.6, the required frame geometry and material properties can be established. Similarly in the case of an RC wall, this can be computed in a similar fashion by modifying the expression in Equation 7 to give

$$\Delta_y = \frac{\sum_{i=1}^{n} m_i \Delta_{y,i}^2}{\sum_{i=1}^{n} m_i \Delta_i} \tag{17}$$

where the yield displacement profile, $\Delta_{y,i}$, is given by

$$\Delta_{y,i} = \frac{\epsilon_y H_i^2}{l_w}\left(1 - \frac{H_i}{3H_n}\right) \tag{18}$$

This results in the same situation where for an RC wall system to have a certain equivalent SDOF yield displacement Δ_y, the required length of wall and material properties can be established. Lastly in the case of braced frames, this may be computed as per Equation 16 above, where only a value of yield drift is needed. In the case of concentrically braced steel frames, this may be computed following Wijesundara et al[37] or O'Reilly and Sullivan[32] for the case of eccentrically braced steel frames.

3.3.8 | Identify design lateral and design system

This last step is relatively straightforward, whereby α_{ULS} is converted to a design base shear, V_b, and distributed along the structure height to result in design member forces as follows:

$$V_b = \alpha_{ULS} m_e = \alpha_{ULS} \frac{\Sigma_{i=1}^{n} m_i \Delta_i}{\Delta_{d,ULS}} \tag{19}$$

The term α_{ULS} can simply be thought of as being approximately equal to the design base shear coefficient, C, since the V_b is found by the product of the effective mass, as shown in Equation 19. These two terms are not exactly equal since the base shear coefficient typically defined as $C = V_b / W = V_b / mg$ which is normalised by the total mass of the structure and acceleration due to gravity, whereas α_{ULS} utilises the effective mass associated with the first mode of response. In structures whose response is dominated by the first mode of response, these two terms will be of similar magnitude meaning that designers may possess a degree of intuition for reasonable initial values of α_{ULS}.

4 | CASE STUDY APPLICATION

Using the design framework summarised in Section 3.1, a case study application is outlined herein. The goal is to define some performance objectives and arrive a set of solutions in terms of structural typology, associated bilinear backbone behaviour, and required structural dimensions. Some of the information required at the various steps may not yet be readily available. In these cases, a reasonable approximation is made in order to illustrate the functionality as opposed to accurate implementation.

4.1 | Identification of building performance requirements

The first step was to identify the site hazard curve, H. For the sake of simplicity, PGA was adopted along with EC8's design spectrum expressions and soil type C was assumed. A simple power-law hazard model given by $H(\text{PGA}) = k_0 \text{PGA}^{k1}$ was adopted where the coefficients k_0 and k_1 were set here to be 5×10^{-5} and 3.0, respectively, for a hypothetical site of moderate seismicity.

Performance objective was identified for a single building occupancy type, where the design EAL was identified to be less than 1.0%. Using the prescribed values of ELR for each limit state outlined in Section 3.2.2, the MAFE of each limit state were determined from Equation 2 and reported in Table 1 along with the assumptions required. To compute the MAFE, dispersions were simply assumed based on judgement for the purposes of illustration and not taken from any specific study, with the values increasing according to the severity of each limit state. Typical values can be found in the literature [eg,[38,39]] for different building typologies and limit state definitions. Furthermore, the chosen values of dispersion are also within the bounds of those recommended in Appendix F of the recent draft of the revised Eurocode 8[24] and are therefore deemed to be suitable for the present scope of illustration. With respect to the target EAL, the design EAL identified shown in Table 1 was computed using a refined curve described by Equation 1 and is verified as being less than 1.0%. This was done by adjusting the design return periods for each limit state until the design EAL was achieved, where the return periods were increased with respect to the values proposed initially in Section 3.2.3. From each of these design limit state return periods, the design PGA was identified using the hazard model above. It is noted that the ULS return period is chosen as 1600 years, which corresponds to the design return period for the significant damage limit state in the revised Eurocode 8. In the case of other design codes with differing minimum design

TABLE 1 Design performance objectives defined by an ELR at each limit state, which were used to compute their respective MAFE and subsequently the design intensities

	OLS	SLS	ULS
y	1%	15%	100%
T_R, years	10	75	1600
H	1.00E−01	1.33E−02	6.25E−04
β	0.1	0.2	0.3
λ	1.05E−01	1.60E−02	9.37E−04
EAL	0.98%		
PGA, g	0.08	0.15	0.38

requirements, such as NZS1170 that requires a design return period of 2500 years at the ultimate limit state, this would also need to be accommodated.

To convert the design loss ratios at both SLS and ULS listed in Table 1 (ie, y_{SLS} and y_{ULS}) into structural design parameters, storey loss functions were required. As outlined in Section 3.2.4, such functions are not widely available yet. Making some reasonable assumptions, the relative storey values for the PSD-sensitive structural and nonstructural and PFA-sensitive nonstructural elements (ie, $Y_{S,PSD}$, $Y_{NS,PSD}$, and $Y_{NS,PFA}$) illustrated in Figure 6 were utilised. Once these were established, all that remained was the definition of expected storey loss for each of the damageable element groups with increasing demand (ie, $y_{S,PSD}$, $y_{NS,PSD}$, and $y_{NS,PFA}$). For simplicity, these were assumed to be linear functions that saturate at the relative repair cost ratio and are illustrated in Figure 11. Knowing the design limit state loss ratios and storey loss functions, the design values of θ_{max} and a_{max} were established from Figure 6 and Equation 4. These values are illustrated in Figure 11, and the more critical design value of θ_{max} was used in each case. Therefore, the building needed to be sized to keep $\theta_{max} \leq 0.98\%$ and $a_{max} \leq 0.32$ g at the SLS, and $\theta_{max} \leq 2.0\%$ at the ULS.

4.2 | Identification of feasible building solutions

Having identified the building performance requirements, this information was used to identify a number of feasible design solutions following the steps outlined in Section 3.1. While Section 4.1 was described without any information regarding building geometry or layout, some basic information was still required. This consisted of the number of storeys, building floor area, and expected loading. For the design scenario outlined herein, a five-storey building with a floor area of 200m^2, seismic floor loading of 8 kPa, and roof loading of 7 kPa was considered.

The identified values of θ_{max} and a_{max} at the SLS then needed to be converted to the spectral accelerations and displacements, $\Delta_{d,SLS}$ and α_{SLS}, respectively. This was outlined in Section 3.3.2, where information regarding the expected displaced shape was required to determine $\Delta_{d,SLS}$ and an approximate conversion factor γ was needed to determine α_{SLS}.

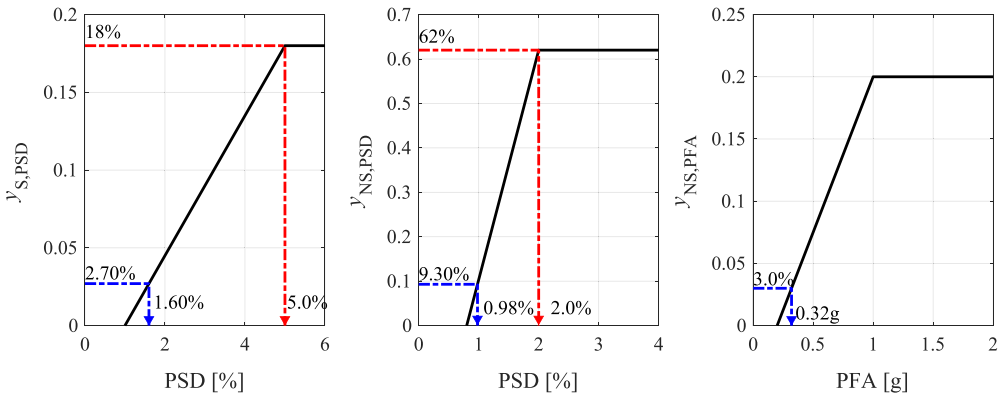

FIGURE 11 Illustration of the storey loss functions, which were assumed to be linearly increasing with respect to demand here for simplicity, and the identification of the design parameters for the SLS (blue) and ULS (red) [Colour figure can be viewed at wileyonlinelibrary.com]

Table 2 lists these values for the three structural systems considered herein. As illustrated in Figure 8, the range of feasible periods were established using the equivalent SDOF spectral limits in Table 2, assuming no nonlinear behaviour at this limit state. By doing so, a permissible initial secant to yield period range (ie, $T_{1,\text{lower}}$ to $T_{1,\text{upper}}$) was found for each structural system, which are listed in Table 3.

To design the structures in the nonlinear range at the ULS, the $\theta_{\max}$ was converted to a spectral displacement similar to step 2 above, where Section 3.3.4 was followed to give a value of $\Delta_{d,ULS}$. The next step in the design process was to trial a value of lateral capacity via the term α_{ULS}. As previously discussed, this term is closely related to the design base shear coefficient and a reasonable starting point would be a value of 0.20 for each typology. By knowing the lateral capacity and permissible period range, the design solution space illustrated in Figure 9 was found (ie, points 1, 2, and 3). These trials of lateral capacity and yield displacement were used to adjust and satisfy the initial secant to yield period constraints to arrive at a suitable design solution. Following Section 3.3.5 and recognising that for a structural system with a reasonable amount of ductility, the DMF was estimated as being around $\eta = 0.60$. This means that the maximum permissible yield displacement that would give this amount of spectral reduction capacity is found via Equation 14 by taking μ as 2.5. This initial estimate was subsequently revised depending on where it fell in the design solution space, but for conceptual design stage, it was deemed a suitable starting point.

These final values of yield displacement and lateral capacity are listed in Table 4 and the required backbone responses plotted in Figure 12. Examining each solution visually, each one falls within their respective design solution spaces, making them all feasible design options. In the case of the braced frame, for example, its design displacement was much larger with respect to the other systems. This was due to its linear displaced shape meaning that it possessed a larger equivalent SDOF system design displacement. As such, it required much less spectral modification capacity via ductility. This therefore meant that the resulting design for the braced frame requires quite a long initial period to satisfy the design constraints. This appears quite odd at first since if the braced frame has been designed using FBD or DDBD for the same design spectra shown in Figure 12, it would likely be a much stiffer building with higher ductility demand. However, it is stressed here that the resulting design determined here is the one that was required to return the expected level of direct monetary losses, since they are the quantity now driving the design process. Therefore, to obtain the expected performance defined in terms of expected losses, the design solution described in Table 4 for the braced frame is required. Briefly commenting on the other two structural systems examined, it can be seen how the final designs fell within the design solution space. Again, further parametric studies are required but the main idea behind the conceptual design procedure ought to be clear. Comparing the design solution for the RC frame and RC wall in Table 4, some interesting observations can be made. Following a more traditional design approach, the period and ductility of the RC frame may have both been expected to have been higher than those of the RC wall. This essentially arises because of the need to respect both the maximum displacements at the ULS and also stay within the permissible initial period range. Therefore, a slightly stronger (in terms of base shear coefficient) RC frame results, which consequently has a lower required ductility and a shorter required initial period. It is worth recalling that RC frames may be typically expected to have longer periods and ductility capacity than RC walls but would also be expected to have higher drift. This is

TABLE 2 Conversion of θ_{max} and a_{max} to spectral values at the DL limit state

	RC Frame	RC Wall	Braced Frame
$\theta_{\max}$, %	0.98%	0.98%	0.98%
ω_θ	1.0	1.0	1.0
$\Delta_{d,SLS}$, m	0.102	0.081	0.124
$a_{\max}$, g	0.32	0.32	0.32
γ	0.60	0.80	0.70
α_{SLS}, g	0.19	0.26	0.22

TABLE 3 Identification of initial secant to yield period range of different structural typologies

	RC Frame	RC Wall	Braced Frame
$T_{1,\text{lower}}$, s	1.31	0.99	1.13
$T_{1,\text{upper}}$, s	1.62	1.29	1.97

TABLE 4 Identification of structural system parameters to respect the design constraints and fall within the design solution space

	RC Frame	RC Wall	Braced Frame
α_{ULS}, g	0.27	0.22	0.21
$\Delta_{d,ULS}$, cm	20.8	20.7	25.3
T_e, s	1.76	1.95	2.20
$Sd\ (T_e)$, cm	28.4	31.4	32.3
$\eta_{required}$	0.73	0.66	0.78
Δ_y, cm	11.84	8.00	19.20
$\mu_{provided}$	1.75	2.59	1.32
T_1, s	1.33	1.21	1.92
V_b, kN	1772.3	1289.4	1313.0
C	0.23	0.17	0.17

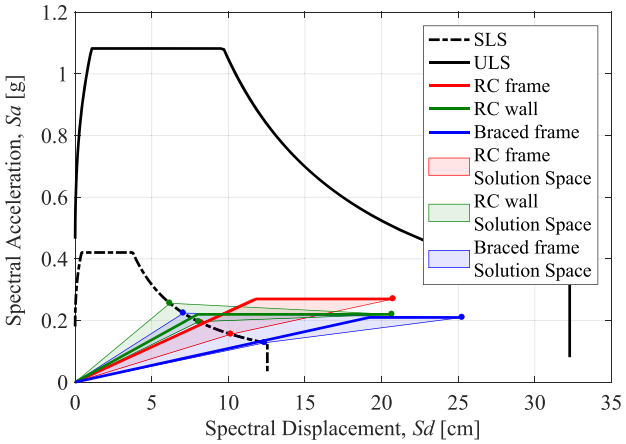

FIGURE 12 Required backbone response for each of the identified design solutions, where the acceptable design solution space in shaded in each case to demonstrate how the design conditions have been respected [Colour figure can be viewed at wileyonlinelibrary.com]

the quantity that needs to be limited as opposed to exploring the full deformation capacity of the structure; hence, the resulting design is required to respect these performance goals rather than maximise the ductility demand. Of course, trialling different values of lateral capacity could potentially increase the ductility demand, but this may adversely impact the initial period of the system.

The previous steps established the feasibility of different structural systems, with Figure 12 indicating the backbone of ones that would lead to an acceptable building performance defined in terms of expected loss. To actually design structures with these backbones, two parameters are required: the lateral strength and the yield displacement. Since the lateral strength is essentially a function of the member strengths, this can be easily adjusted by modifying the dissipative zone capacities. To establish the yield displacement, the structural geometry and material properties were required. However, since the required yield displacement was known, Section 3.3.7 was used to determine the suitable structure geometry. Considering an RC wall system, for example, the structural geometry was identified and for it to function, an RC wall length, l_w, of 4.5 m would be required, assuming a reinforcement of yield strength 500 MPa. Similarly in the case of the RC frame system, a frame with 0.50- m deep beams and a bay width of 5.5 m would be required, assuming a similar grade of reinforcement. For a braced frame system, a concentrically braced steel frame could be utilised with a bay width of 17.9 m. As previously noted, this bay width may be deemed too large and unfeasible meaning that such a structural system may be discarded from the list of potential design systems. Alternatively, it may be an indication of where other measures such as base isolation and/or supplemental dampers may be further investigated in conjunction with the braced frame. This highlights one of the key aspects of the proposed framework, where unfeasible systems such as a braced frame in this case can be identified as being difficult to design for within a performance-based design framework.

Knowing the lateral load-resisting system, structural geometry, and the design base shear for the system using Equation 19, the structure can be designed and detailed, ensuring the relevant detailing and capacity design requirements to ensure a ductile and stable mechanism. The result of this would be that the structural system designed in this manner would be representative the backbone identified in Figure 12 and would satisfy the building performance goals initially defined in terms of EAL. The actual provision of this performance may be subsequently verified using an assessment procedure such as that outlined Figure 1 but is deemed beyond the scope of this article.

5 | DISCUSSION

5.1 | Comparison with existing design codes

Examining the proposed framework, a number of improvements can be noted with respect to the limitations of current code prescriptions discussed in Section 2.1. Current codes give relatively little explicit consideration to limit states other than the life safety requirement. Some checks may be present for nonstructural elements at lower return periods but are widely known to be insufficient. Furthermore, the mitigation of excessive floor accelerations to protect nonstructural elements and building contents is generally not given direct consideration. With respect to these limitations, the proposed design framework is a clear progression. It considers both drift and acceleration-sensitive elements at the SLS by identifying a suitable initial secant to yield period range.

Consider another aspect where a building's structural system is first identified and subsequently sized; the proposed framework is a significant improvement in this regard. The desired backbone performance is identified, and the required structural geometry subsequently established. This is because the yield displacement of a system can be related back to structural dimensions and is relatively independent of the lateral strength. This follows on from the initial thinking outlined by Priestley et al[11]; the assumption of constant lateral stiffness for variations of the same typology in FBD was demonstrated to be illogical, and it was, in fact, the yield displacement that tended to remain constant.

5.2 | Comparison with other PBEE methodologies

Compared with other methodologies in the literature with a similar scope, two specific developments come to mind. The first of these is the decision support framework (DSF)[17] and the yield frequency spectra (YFS) method.[40] Compared with the DSF, the proposed framework bares some similarities since it uses expected loss along with storey loss functions. This main difference, and advancement proposed here, is that the DSF method requires extensive numerical modelling and simulation of a building that has yet to be designed, combining each of the three phases of seismic design at once. The proposed approach focuses on the first phase of conceptual design and utilises simplifying assumptions to provide a good starting point that may be eventually followed with more rigorous verification and refinement. This YFS method is a convenient method to ensure a risk-consistent design by capitalising on the stability of the yield displacement to identify a suitable backbone behaviour, similar to the proposed approach. Both methods utilise an equivalent SDOF system to characterise the structural response, but the principal difference is that the proposed framework utilises expected monetary losses from the outset of design, whereas the YFS method uses structural ductility. Ductility is a pertinent parameter in seismic performance but is arguably not of paramount interest when considering structural and also nonstructural damage in the broader scope of PBEE. Therefore, the proposed method aims to focus more on EAL by limiting storey drift and floor acceleration. This is not necessarily a limitation of the YFS method, but rather a difference in the initial objectives of design since the basic formulation of the YFS method is quite similar to the proposed method and could certainly be extended in a similar manner.

5.3 | Base isolation and supplemental damping

While not discussed here, one area the proposed framework can be of great benefit to practitioners is in relation to the decision to use base isolation or supplemental damping. This is something very often decided by the engineer based on experience or as result of difficulty in finding a feasible solution following some initial analysis. In the proposed framework, this would be more direct and obvious to designers because of the way performance objectives are set out. Consider those utilised in Section 3.3.2 for the SLS marked in Figure 13. If the case arose where the SLS demand was too

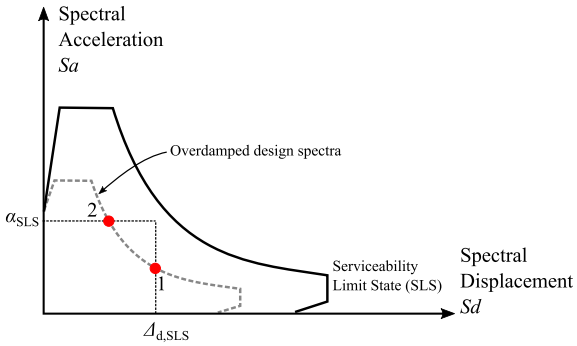

FIGURE 13 Example of when SLS performance objectives cannot be met, and some solution in the form of base isolation or supplemental damping is required [Colour figure can be viewed at wileyonlinelibrary.com]

large and a suitable period range could not be identified via an intersection with the design spectrum, this would be an indication of a situation where additional measures may be required. This is because it is not possible for traditional systems to mitigate the displacements and accelerations at the SLS, whereas base isolation or supplemental damping would reduce this design demand and permit more feasible solutions to be found. These aspects are to be developed further in future studies.

5.4 | Limitations and future developments

The proposed design framework outlines how feasible structural systems may be identified to meet the targeted performance defined in terms of EAL. However, some limitations of the framework are noted in addition to future developments. First, relating the ELR to the required design value of θ_{max} or a_{max} shown in Figure 6 inherently assumed that constant demands are over the entire building height, as illustrated in Figure 14, but from Figure 7, can be seen not to be the case. This means that during a subsequent design verification using the same storey loss functions, the ELR at each limit state would be slightly reduced. This can be rectified and refined at a later stage but is in any case noted to be a conservative assumption whose impact will diminish for structures with more uniform distributions of demand.

Another limitation and future development would be to consider indirect losses in the proposed design framework. The ELR values discussed in Section 3.2.2 referred exclusively to direct loss since y_{ULS} was set at 100% of the building replacement cost. Indirect losses may be incorporated through a more advanced ELR definition depending on the building occupancy type and its strategic role in society. For example, consider the total losses observed in a hypothetical building like a hospital in Figure 15. At the OLS, no indirect losses are anticipated and the total loss comprises solely the direct loss. With increasing damage to the building, the indirect losses begin to accumulate because of issues like having to set up temporary shelters or potentially move patients to another facility at the SLS and ULS. Beyond the ULS, the direct losses will saturate, but the indirect losses may markedly increase due to the complete structural

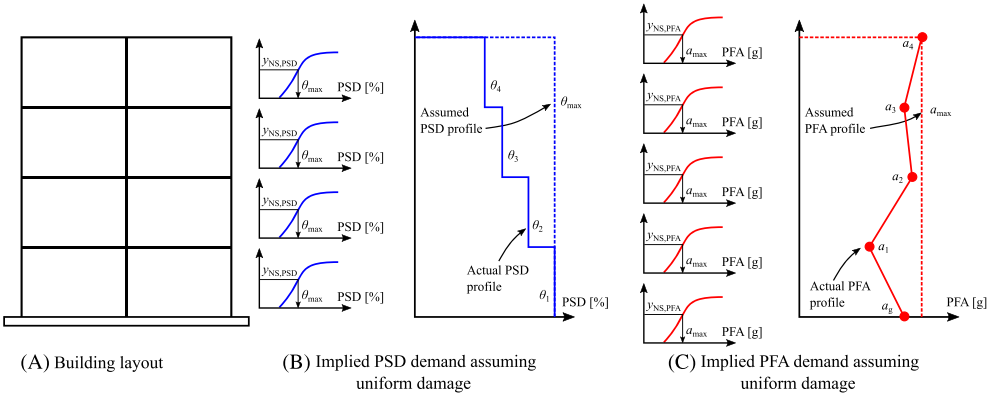

FIGURE 14 Limitation of proposed design framework where design EAL tends to be overestimated due to simplifying assumption regarding the building demand distribution along height [Colour figure can be viewed at wileyonlinelibrary.com]

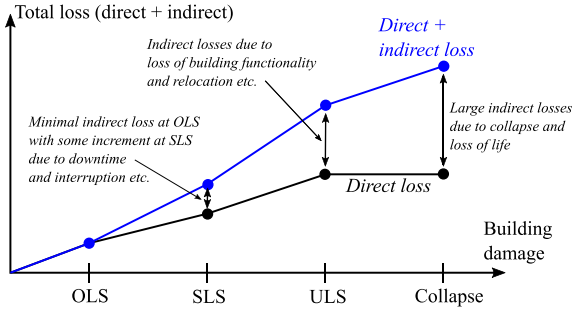

FIGURE 15 Evolution of total losses with increasing building damage, where potential sources of indirect losses are indicated with respect to the building damage. (Vertical axis not to scale) [Colour figure can be viewed at wileyonlinelibrary.com]

collapse and loss of life, for example. Considering these aspects, the losses associated with each limit state in Figure 4 and the target EAL may be adjusted to consider indirect losses at the design stage. In current design codes, importance factors are typically used meaning that the seismic input is amplified by a fixed coefficient to provide increased lateral resistance. It is argued that considering the importance of a building using total losses may be a more comprehensive and somewhat integrated approach.

6 | SUMMARY

A novel design framework utilising EAL to identify feasible structural solutions that align with the conceptual goals of performance-based design has been outlined. It is intended to form the first phase in the design process where the building is conceptually designed before being later detailed and verified with more detailed analysis. As with any simplified method, a number of assumptions were needed. The first of these was the use of storey loss functions to convert expected loss ratios to design peak storey drift, θ_{max}, and peak floor acceleration, a_{max}. Two limit state intensities, serviceability (SLS) and ultimate limit states (ULS), were considered to characterise the structure's initial elastic and ductile nonlinear behaviour. For the SLS, it was shown how θ_{max} and a_{max} can be used to characterise a permissible initial secant to yield period range. By trialling a lateral resistance and knowing the required system ductility for the ULS, the yield displacement of the system can be computed. Considering this with the acceptable period range, the design solution space can be identified and a potential bilinear backbone identified. Knowing that a structure's yield displacement depends primarily on material properties and geometry, the required dimensions of the structure can be identified as part of the first phase of design where the structural system and its layout are conceived. A case study example of the design framework was subsequently outlined to illustrate its application, where the relative simplicity and ease at arriving at feasible solutions were demonstrated.

ACKNOWLEDGEMENTS

The work presented in this paper has been developed within the framework of the project "Dipartimenti di Eccellenza", funded by the Italian Ministry of Education, University and Research at IUSS Pavia. The authors would like to thank Prof. Dimitrios Vamvatsikos for his valuable comments and suggestions.

ORCID

Gerard J. O'Reilly https://orcid.org/0000-0001-5497-030X
Gian Michele Calvi http://orcid.org/0000-0002-0998-8882

REFERENCES

1. SEAOC. *Vision 2000: Performance-based seismic engineering of buildings*. Sacramento, California: Structural Engineers Association of California; 1995.

2. EN 1998–1:2004. *Eurocode 8: Design of Structures for Earthquake Resistance - Part 1: General Rules, Seismic Actions and Rules for Buildings*. Brussels, Belgium: 2004.
3. ASCE 7–16. *Minimum Design Loads for Buildings and Other Structures*. Reston, VA, USA: 2016.
4. NZS 1170.5:2004. *Structural Design Actions Part 5: Earthquake Actions - New Zealand*. Wellington, New Zealand: 2004.
5. Cornell CA, Krawinkler H. Progress and challenges in seismic performance assessment. *PEER Center News*. 2000;3(2):1-2.
6. FEMA P58–1. *Seismic Performance Assessment of Buildings: Volume 1—Methodology (P-58-1)*. vol. 1. Washington, DC: 2012.
7. O'Reilly GJ, Perrone D, Fox M, Monteiro R, Filiatrault A. Seismic assessment and loss estimation of existing school buildings in Italy. *Eng Struct*. 2018;168:142-162. https://doi.org/10.1016/j.engstruct.2018.04.056
8. Luco N, Ellingwood BR, Hamburger RO, Hooper JD, Kimball JK, Kircher CA. Risk-Targeted versus Current Seismic Design Maps for the Conterminous United States. SEAOC 2007 Convention, 2007.
9. Vamvatsikos D. Performance-based seismic design in real life: the good, the bad and the ugly. In: *ANIDIS 2017*. Pistoia, Italy; 2017.
10. Priestley MJN. Myths and fallacies in earthquake engineering, revisited. In: *The 9th Mallet Milne Lecture*. Pavia, Italy: IUSS Press; 2003.
11. Priestley MJN, Calvi GM, Kowalsky MJ. *Displacement Based Seismic Design of Structures*. Pavia, Italy: IUSS Press; 2007.
12. Taghavi S, Miranda E. Response assessment of nonstructural building elements. PEER Report 2003/05 2003.
13. Welch DP, Sullivan TJ. Nonstructural considerations for seismic serviceability performance in European steel moment frames. In: *Giornate Italiane della Costruzione in Acciaio*. Torino, Italia; 2013.
14. Vamvatsikos D, Kazantzi AK, Aschheim MA. Performance-based seismic design: Avant-Garde and code-compatible approaches. *ASCE-ASME Journal of Risk and Uncertainty in Engineering Systems, Part a: Civil Engineering*. 2016;2(2):C4015008. https://doi.org/10.1061/AJRUA6.0000853
15. Decreto Ministeriale. *Linee Guida per la Classificazione del Rischio Sismico delle Costruzioni - 58/2017*. Rome, Italy: 2017.
16. Calvi GM, Sullivan TJ, Welch DP. A seismic performance classification framework to provide increased seismic resilience. *2nd European Conference on Earthquake Engineering and Seismology*, Istanbul, Turkey: 2014.
17. Krawinkler H, Zareian F, Medina RA, Ibarra LF. Decision support for conceptual performance-based design. *Earthquake Engineering & Structural Dynamics*. 2006;35(1):115-133. https://doi.org/10.1002/eqe.536
18. Calvi GM. Revisiting design earthquake spectra. *Earthquake Engineering & Structural Dynamics*. 2018;47(13):2627-2643. https://doi.org/10.1002/eqe.3101
19. Dolce M, Manfredi G. *Libro bianco sulla ricostruzione privata fuori dai centri storici nei comuni colpiti dal sisma dell'Abruzzo del 6 aprile 2009*. Doppiavoce, Napoli, Italy:2015.
20. Welch DP, Sullivan TJ, Calvi GM. Developing direct displacement-based procedures for simplified loss assessment in performance-based earthquake engineering. *Journal of Earthquake Engineering*. 2014;18(2):290-322. https://doi.org/10.1080/13632469.2013.851046
21. Vamvatsikos D. Derivation of new SAC/FEMA performance evaluation solutions with second-order hazard approximation. *Earthquake Engineering & Structural Dynamics*. 2013;42(8):1171-1188. https://doi.org/10.1002/eqe.2265
22. O'Reilly GJ, Sullivan TJ. Probabilistic seismic assessment and retrofit considerations for Italian RC frame buildings. *Bulletin of Earthquake Engineering*. 2018;16(3):1447-1485. https://doi.org/10.1007/s10518-017-0257-9
23. RINTC Workgroup. Results of the 2015-2017 Implicit seismic risk of code- conforming structures in Italy (RINTC) project. ReLUIS Report 2018.
24. Cornell CA, Jalayer F, Hamburger RO, Foutch DA. Probabilistic basis for 2000 SAC Federal Emergency Management Agency steel moment frame guidelines. *Journal of Structural Engineering*. 2002;128(4):526-533. https://doi.org/10.1061/(ASCE)0733-9445(2002)128:4(526).
25. Pinto PE, Franchin P. Existing buildings: The New Italian Provisions for Probabilistic Seismic Assessment. In: Ansal A, ed. *Perspectives on European Earthquake Engineering and Seismology*. Springer; 2014 https://doi.org/10.1007/978-3-319-07118-3.
26. EN 1998–1:2018. *Eurocode 8: Design of Structures for Earthquake Resistance (Draft) - Part 1: General Rules, Seismic Actions and Rules for Buildings*. Brussels: 2018.
27. Ramirez CM, Miranda E. Building specific loss Estimation Methods & Tools for simplified performance based earthquake engineering. *Blume Report No 171* 2009.
28. Papadopoulos AN, Vamvatsikos D, Kazantzi AK. Development and application of FEMA P-58 compatible story loss functions. *Earthq Spectra*. 2018. https://doi.org/10.1193/020518EQS033M.
29. Calvi PM, Sullivan TJ. Estimating floor spectra in multiple degree of freedom systems. *Earthq Struct*. 2014;7(1):17-38. https://doi.org/10.12989/eas.2014.7.1.017
30. Miranda E. Inelastic displacement ratios for structures on firm sites. *J Struct Eng*. 2000;126(10):1150-1159. https://doi.org/10.1061/(ASCE)0733-9445(2000)126:10(1150).

31. Vidic T, Fajfar P, Fischinger M. Consistent inelastic design spectra: strength and displacement. *Earthq Eng Struct Dyn*. 1994;23(5):507-521. https://doi.org/10.1002/eqe.4290230504
32. O'Reilly GJ, Sullivan TJ. Direct displacement-based seismic design of eccentrically braced steel frames. *J Earthq Eng*. 2016;20(2):243-278. https://doi.org/10.1080/13632469.2015.1061465
33. Dwairi HM, Kowalsky MJ, Nau JM. Equivalent damping in support of direct displacement-based design. *J Earthq Eng*. 2007;11(4):512-530. https://doi.org/10.1080/13632460601033884
34. Blandon CA, Priestley MJN. Equivalent viscous damping equations for direct displacement based design. *J Earthq Eng*. 2005;9(sup2):257-278. https://doi.org/10.1142/S1363246905002390
35. Pennucci D, Sullivan TJ, Calvi GM. Displacement reduction factors for the design of medium and long period structures. *J Earthq Eng*. 2011;15(Supp 1):1-29. https://doi.org/10.1080/13632469.2011.562073
36. Miranda E, Ruiz-García J. Evaluation of approximate methods to estimate maximum inelastic displacement demands. *Earthq Eng Struct Dyn*. 2002;31(3):539-560. https://doi.org/10.1002/eqe.143
37. Wijesundara KK, Bolognini D, Nascimbene R, Calvi GM. Review of design parameters of concentrically braced frames with RHS shape braces. *J Earthq Eng*. 2009;13(sup1):109-131.
38. Kosič M, Dolšek M, Fajfar P. Dispersions for the pushover-based risk assessment of reinforced concrete frames and cantilever walls. *Earthq Eng Struct Dyn*. 2016;45(13):2163-2183. https://doi.org/10.1002/eqe.2753
39. O'Reilly GJ, Sullivan TJ. Quantification of modelling uncertainty in existing Italian RC frames. *Earthq Eng Struct Dyn*. 2018;47(4):1054-1074. https://doi.org/10.1002/eqe.3005
40. Vamvatsikos D, Aschheim MA. Performance-based seismic design via yield frequency spectra. *Earthq Eng Struct Dyn*. 2016;45(11):1759-1778. https://doi.org/10.1002/eqe.2727

How to cite this article: O'Reilly GJ, Calvi GM. Conceptual seismic design in performance-based earthquake engineering. *Earthquake Engng Struct Dyn*. 2019;48:389–411. https://doi.org/10.1002/eqe.3141